

# A Methodology for Realizing High Efficiency Class-J in a Linear and Broadband PA

Peter Wright, Jonathan Lees, Johannes Benedikt, Paul J. Tasker, *Senior Member, IEEE*, and Steve C. Cripps

**Abstract**—The design and implementation of a class-J mode RF power amplifier is described. The experimental results indicate the class-J mode's potential in achieving high efficiency across extensive bandwidth, while maintaining predistortable levels of linearity. A commercially available 10 W GaN (gallium nitride) high electron mobility transistor device was used in this investigation, together with a combination of high power waveform measurements, active harmonic load-pull and theoretical analysis of the class-J mode. Targeting a working bandwidth of 1.5–2.5 GHz an initial power amplifier (PA) design was based on basic class-J theory and computer-aided design simulation. This realized a 50% bandwidth with measured drain efficiency of 60%–70%. A second PA design iteration has realized near-rated output power of 39 dBm and improved efficiency beyond the original 2.5 GHz target, hence extending efficient PA operation across a bandwidth of 1.4–2.6 GHz, centered at 2 GHz. This second iteration made extensive use of active harmonic load-pull and waveform measurements, and incorporated a novel design methodology for achieving predistortable linearity. The class-J amplifier has been found to be more realizable than conventional class-AB modes, with a better compromise between power and efficiency tradeoffs over a substantial RF bandwidth.

**Index Terms**—Broadband, class-J, high efficiency, power amplifiers.

## I. INTRODUCTION

**P**OWER AMPLIFIER (PA) design for wireless communication has, until recently, been focused on specified RF bandwidths of 5% or lower, due mainly to the very tight spectrum allocations. Future systems, including WiMax, 4G, and beyond, will likely require larger bandwidths, not just due to wider spectral allocations, but the base bandwidth of the signals themselves which may well extend up to, and ultimately exceed, 100 MHz. To date, other RF power amplifier (RFPA) applications, such as radar and environmental climate monitoring (ECM) have not profited from advances in power and efficiency due to their much wider RF bandwidth requirements. Reported results on very high efficiency PAs, typically operating above 75% efficiency, tend to rely heavily upon precise multi-harmonic impedance terminations at the

device-under-test (DUT) as well as very high levels of device gain-compression. Both of these factors lead to narrowband frequency performance limitations (less than 10%) and non-linear operation, respectively. A newly presented, and much discussed, mode of operation—class-J [1]—has shown the theoretical potential of obtaining linear RFPAs that have the same efficiency and linearity as conventional class-AB designs but do not require a band-limiting transmission-line harmonic short. The class-J mode uses second harmonic voltage enhancement, as described by previous workers [1]–[5]. This technique poses an immediate problem inasmuch as the device absorbs, rather than generates, second harmonic power. Techniques such as current waveform clipping [2], or wave-shaping the input signal [3] have been proposed in an attempt to null the second harmonic component. The class-J approach utilizes a phase shift between the output current and voltage waveforms to render the second harmonic termination into the purely reactive regime. This enables significant possibilities into the realizable bandwidth-efficiency performance of the class-J mode of PA using GaN high electron mobility transistor (HEMT) power transistors.

This paper follows on from research presented in [4] and describes some of the key results obtained in that work in which design and realization of PA matching networks has yielded a broadband amplifier operating at high efficiency. In addition, application of a new theory [5], from which a furthering of the novel broadband class-J design methodology has been made, is presented and an enhanced PA design realized with increased relative bandwidth-efficiency. This second and new design iteration makes comprehensive use of active load-pull, or “waveform engineering” techniques, and uses a novel design methodology to achieve predistortable linearity [6], [7]. To our knowledge, such a design has never before been attempted on an *a priori* basis.

The high power measurement and characterization capability at our facility [8] has been utilized in the development of this broadband PA design methodology, demonstrating a new practical approach to handling the second harmonic loading problem in broadband PA designs. Work such as in [9], which addresses multi-octave high efficiency PA designs, use resistive second harmonic loading within a portion of the specified bandwidth. Hence (and appropriately), only fundamental load optimization is considered viable in such cases. This paper presents research enabling a good compromise in efficiency across bandwidths below one octave.

Waveform and systematic load-pull measurement data has been used in the development stage of the design procedure, whilst also being used to analyze the extent to which optimum

Manuscript received May 05, 2009; revised September 10, 2009. First published November 03, 2009; current version published December 09, 2009. This work was supported in part by Milmega Ltd. and in part by the Engineering and Physical Sciences Research Council (EPSRC).

The authors are with the Centre for High Frequency Engineering, Cardiff School of Engineering, Cardiff University, CF24 3AA Cardiff, U.K. (e-mail: wrightp@cardiff.ac.uk; leesj2@cardiff.ac.uk; spejb2@groupwise.cf.ac.uk; tasker@cardiff.ac.uk; stevehywave@aol.com).

Color versions of one or more of the figures in this paper are available online at <http://ieeexplore.ieee.org>.

Digital Object Identifier 10.1109/TMTT.2009.2033295

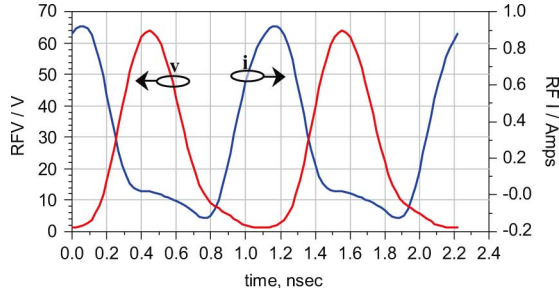


Fig. 1. Measured typical class-J waveforms on a 10 W GaN HEMT [4].

broadband high-efficiency operation has been achieved in this mode. Measurements have been focused around a target sub-octave bandwidth of 1.5–2.5 GHz.

Device output parasitic de-embedding has been applied to the waveforms captured at the calibrated measurement plane of the device package in confirming class-J behavior from the output voltage and current waveforms at the device plane [10].

## II. CLASS-J MODE OF OPERATION

### A. Class-J Harmonic Load Terminations

Cripps [1], who acknowledges some earlier work by Raab [11] has described class-J, defined as a mode in which the voltage has harmonic components which make it tend asymptotically towards a half-wave rectified sine-wave. This in practice can be usefully approximated by a suitably phased second harmonic component. The key difference between class-J and more familiar class-A, AB and F modes, is the requirement for a reactive component at the fundamental load. The differentiation between class-J and class-E has been explained in detail in [1] and cited elsewhere in [12], and can be considered the starting condition in each case. The starting point in class-J design methodology is the linear class-B (or “deep” class-AB) mode, where the output current waveform is a classical reduced conduction angle sinusoid. As such, the class-J amplifier can be expected to have the same linear performance as a class-AB amplifier operating at the same conduction angle. The starting point for a class-E mode (i.e., [13]), however, is to assume that the active device behaves as an ideal switch. Thus any practical implementation of a class-E design requires that the active device be “forced” into behaving like a switch, and this usually involves the device being forced to clip on the supply rails for a part of the RF cycle. This leads to strongly nonlinear performance, albeit often with very high efficiency.

The class-J voltage waveform is “engineered” by using appropriate passive fundamental and second harmonic terminations. In this way, a higher fundamental component can significantly outweigh the loss in power implied by the reactive load, a counter-intuitive result that has been discussed in detail elsewhere [1]. A class-J design thus displays approximate half-wave rectified sinusoidal output current and voltage waveforms, with a phase overlap between the two (see Fig. 1). This mode of operation lends itself very well to the process of waveform engineering, as described previously by some of the current au-

TABLE I  
IDEAL CLASS-J VOLTAGE WAVEFORM, ASSUMING TWO HARMONICS

Harmonic	Normalized voltage component
1	1.41 $\angle 45^\circ$
2	0.50 $\angle -90^\circ$

TABLE II  
CLASS-J  $I_{GEN}$  (CURRENT GENERATOR)-PLANE LOAD TERMINATIONS

Frequency	$I_{gen}$ -Plane Load Impedance
$f_0$	43.8 + j45.2 $\Omega$
$2f_0$	1.6 - j52.0 $\Omega$
$3f_0$	2.4 - j49.7 $\Omega$

thors [8], [14]. Independent bias and drive control, and active multi-harmonic load-pull are used to engineer the shape of the current and voltage waveforms, respectively.

The class-J output voltage waveform—assuming two-harmonics—is specified in Table I [1]. From this the fundamental and second-harmonic impedances, as defined in (1) and (2), can be found, thus defining the matching criteria. In order to optimize efficiency, the GaN device requires some compromises in setting the design values for the fundamental (“load-line”) resistance, due to the potential walkout effect at RF of the dc “knee”-voltage offset [15]

$$Z_{f_0} = R_L + j \cdot R_L \quad (1)$$

$$Z_{2f_0} = 0 - j \cdot \frac{3\pi}{8} \cdot R_L. \quad (2)$$

Ideal class-J theory assumes that there is no third-harmonic component present in the voltage waveform, and hence  $Z_{3f_0}$  is assumed short. This required loading can usually be readily approximated through the effect of the device output capacitance within a PA matching network design, which thus has the tendency to provide a short to all of the higher harmonics. Fig. 1 illustrates measured waveforms with these harmonic terminations, however in this measurement the third harmonic load was allowed to be adjusted slightly in order to demonstrate optimum class-J waveforms and hence, high power and efficiency (as specified in Table II). The bias point implemented here was deep class-AB ( $I_{dq} \approx 5\%$  of  $I_{dss}$ ).

### B. Waveform Engineering Very High Efficiency Class-J Operation in a GaN HEMT

By applying the prescribed class-J impedance components up to  $3f_0$ , through active load-pull, very high efficiency device operation has been measured at a fundamental frequency of 1.8 GHz. The power sweep for this optimum emulated case is shown in Fig. 2. This shows the output performance of the DUT in a class-J loading configuration, operating with a bias point in class-C.

In this separate attempt to demonstrate the very high efficiency potential of class-J, this condition saw the conduction angle reduced beyond the class-B starting point, to the detriment of the device output power.

A peak drain efficiency of 83% has been measured in this state with just below 10 W device output power and approximately 3.5 dB of gain compression. Note that even at the 6 dB power

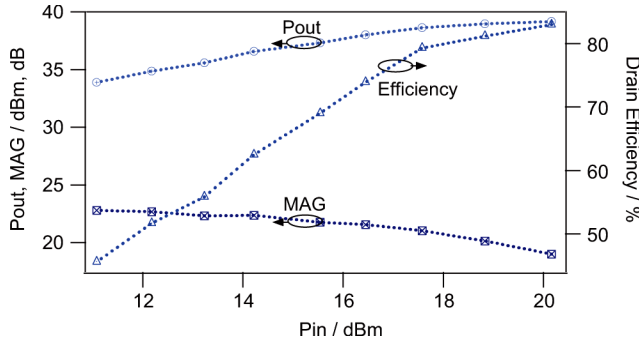


Fig. 2. Power sweep showing very high efficiency class-J operation at 1.8 GHz [input unmatched, maximum available gain (MAG) shown] [4].

back-off point, the measured drain efficiency is still above 60%. Device output power is however slightly less than was observed for the same device type in an optimized class-F/class-F<sup>-1</sup> PA mode, within the same boundary conditions [14].

Following this initial performance characterization of the class-J mode, a linear 10 W broadband PA design was initiated, with a goal of above 60% efficiency over the 50% bandwidth of 1.5–2.5 GHz.

### III. BROADBAND LINEAR CLASS-J PA DESIGN

#### A. Broadband Measurements and PA Realization

Active harmonic load-pull was initiated on the GaN transistor to be used in the design, using the three-harmonic active load-pull setup [8]. This was carried out at several frequencies between 1.5 and 2.3 GHz in order to begin the design stage of the broadband class-J PA. The device was set in the same state of gain compression (approximately P2 dB) in each class-J measurement scenario. Working with device measurement data at the calibrated package-plane (i.e., without output parasitic de-embedding applied) the resulting load-pull sweep data was used to map out the drain efficiency as a function of fundamental load impedance on the Smith chart, with the second and third harmonic impedances fixed according to the ideal class-J terminations stated in Section II-A.

Fig. 3 shows the 70% drain efficiency contour obtained from each fundamental load sweep, indicating the movement of the optimum fundamental load for efficiency at the device package-plane as a function of frequency. A corresponding output power contour plot was extracted following the load-pull sweep which provided a “target region” of load impedances for which to aim a matching circuit design to provide a compromised class-J PA output power and drain efficiency.

The original target frequency band was 1.5–2.5 GHz and in designing a suitable matching network over this extended bandwidth, some compromises have to be made. The initial strategy on the first design iteration (presented in this section) was to give higher priority to the fundamental impedance and allow the second harmonic more latitude. This particular device has a low output capacitance (approximately 1.5 pF) which at 2 GHz is itself quite close to the optimum reactive termination at the second harmonic. Thus the network itself mainly synthesizes the required fundamental load over the extended bandwidth, but

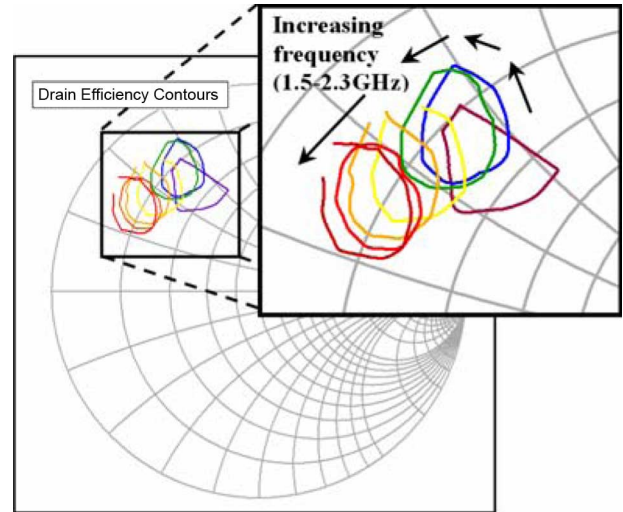


Fig. 3. Measured load-pull data for GaN HEMT indicating load impedance contour for 70% P2 dB drain efficiency between 1.5–2.3 GHz [4].

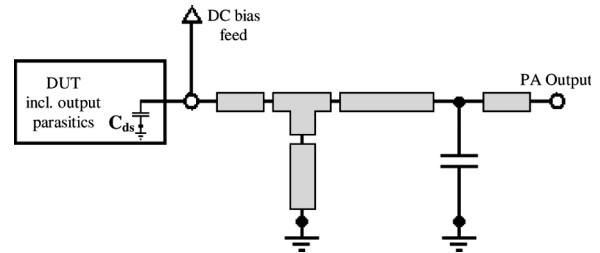


Fig. 4. Realized load matching network schematic [1].

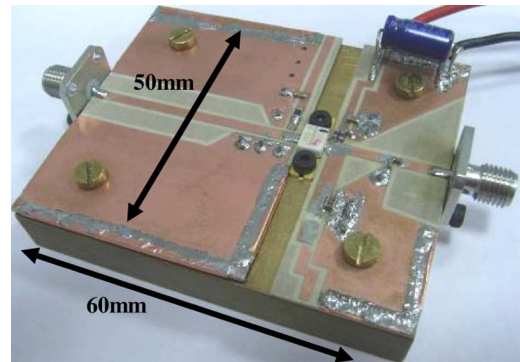


Fig. 5. Realized class-J amplifier—output matched only.

through a shunt inductive stub increases the effective second harmonic capacitive reactance for lower frequencies.

The output matching network schematic is shown in Fig. 4. Although not a novel architecture in itself (variations of this network are analyzed, for example, in [16]), this structure was found, somewhat empirically, to provide the broadband fundamental and second harmonic loading required, enabling a demonstration of the potential as a prototype PA for the emulated broadband operation already carried out. For purposes of comparison between the load-pull emulation and the realized PA performance, the same 50- $\Omega$  input impedance environment was used.

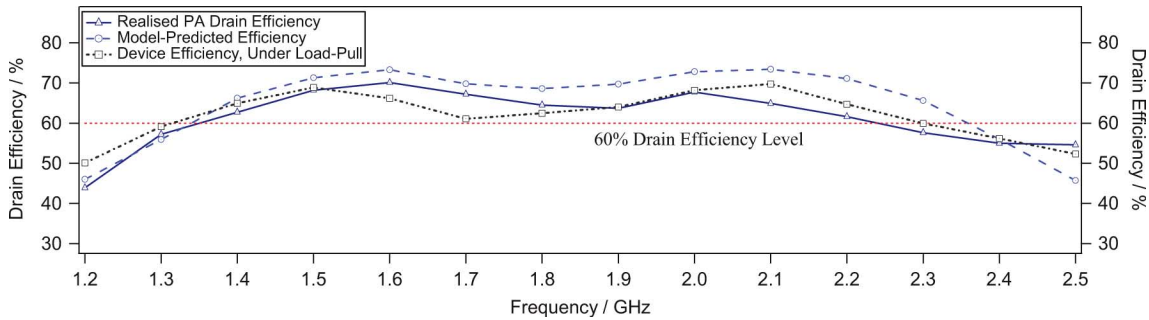


Fig. 6. P2 dB drain efficiency for device under load-pull, model-simulation and realized class-J PA (input unmatched) across a bandwidth of 1.2–2.5 GHz.

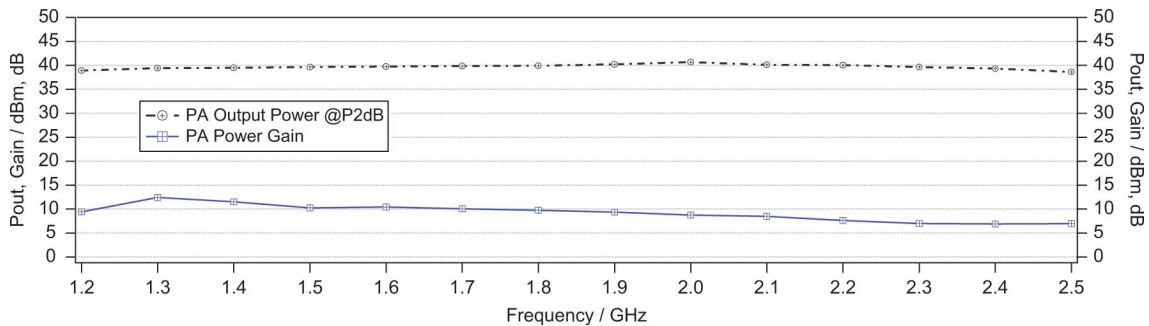


Fig. 7. Realized class-J PA output power and PA power gain (input unmatched, i.e., 50  $\Omega$ ) at P2 dB across bandwidth of 1.2–2.5 GHz.

### B. Realized Class-J Performance Results—Efficiency and Output Power Versus Frequency

The first realized design iteration of the class-J amplifier is shown in Fig. 5. Power sweeps over a 12 dB range were carried out on the PA across a frequency range of 1.2–2.5 GHz. Results of this sweep are shown in Figs. 6 and 7. The efficiency performance at the P2 dB compression state is displayed; this is customarily used as an “end-point” for useable high-end efficiency performance in high peak-to-average ratio (PAR) linear signal applications.

As seen in Fig. 6, the measured P2 dB drain efficiency for the realized class-J amplifier is at a level of 60%–70% between 1.35 and 2.25 GHz; a 50% bandwidth about a center frequency of 1.8 GHz. Within this bandwidth corresponding output power from the amplifier is between 9 and 11.5 W.

A comparison between the realized PA results and simulated efficiency from the nonlinear device model, set in the same impedance environment, is also shown in Fig. 6.

### C. Analysis of Measured PA Performance

The results from this realized class-J design show a wide bandwidth of high efficiency operation; however the optimum performance is not obtained all of the way to the top end of the initially desired 1.5–2.5 GHz bandwidth, i.e., above 2.2 GHz, efficiency and output power begin to roll off. Using the active harmonic load-pull test setup to present the same impedance environment as the PA (up to the second harmonic), a verification of the expected performance could be ascertained, as in Fig. 6, allowing for further investigation into the reasons for the reduced performance, and hence indicate actions to take in order to improve the high-end performance.

The load-pull results—in which the fundamental and second harmonic load impedances were presented to the device—highlights the same trend in device drain efficiency, in particular the drop in efficiency above 2.2 GHz.

By introducing refinements in the basic class-J theory [5] into the design approach, a new enhanced design was made, aimed not only at improving the high-end efficiency and output power, but also addressing linearity, and potentially, predistortability.

## IV. CLASS-J LINEARITY AND CLIPPING ANALYSIS

### A. Wider Bandwidth Potential of the Class-J Mode

As shown in [5], the “class-J mode” encompasses a continuum of high efficiency performance modes, each with a reactively terminated second harmonic load. The fundamental load has to have a corresponding reactive component in order to maintain a “positive-definite,” or non-zero-crossing voltage waveform. This continuum applies for second harmonic capacitive reactance terminations up to the short-circuit condition for class-B, and extends beyond this point towards what is denoted as the class-J\* mode [5], i.e., the conjugates of the class-J loads in (1) and (2).

It is therefore possible to utilize this “design-space” to implement an amplifier which has comparable efficiency, power and linearity performance as is regularly obtained using conventional class-AB design methodology, but retains almost constant performance over a substantially extended bandwidth. To our knowledge, such a design has never before been attempted on an *a priori* basis.

### B. Use of “Clipping Contours” for Quasi-Linear Design

The device output voltage,  $V_o$ , in a class-J PA can be written in the form [5]

$$V_o(\theta) = V_{dc} - V_{1r} \cos \theta + V_{1q} \sin \theta + \sum_n V_{nq} \sin(n\theta), \quad (\theta = \omega t) \quad (3)$$

where in this case  $n = 2$ , and  $r$  and  $q$  denote the real and quadrature voltage components, respectively.

If the minimum value of  $V_o$  approaches the device “knee” ( $v_{\min}$ ) at any point in the RF cycle, the device current will start to “clip,” resulting in highly nonlinear behavior. Such clipping will clearly cause gain compression, or AM–AM distortion, and if there is a significant phase angle between the fundamental components of current and voltage it is, in addition, a primary cause of AM–PM distortion. These strongly nonlinear effects not only cause spectral distortion but can also lead to increasing problems when attempting to linearize the device using input signal predistortion.

It is therefore of much relevance to examine the parametric dependency of the “zero-crossing” behavior of the voltage expression in (3). Even with the convenient approximation,  $v_{\min} = 0$ , this is a mathematical problem of some complexity which we have analyzed in more detail elsewhere [5]. But for the present purpose it is possible to transform the clipping expression into a more simple graphical representation. If we assume that the current waveform remains a classical reduced-conduction-angle class-AB form, the voltage parameters  $V_{1r}$ ,  $V_{1q}$ , and  $V_{2q}$  in (3) can be considered to be directly proportional to the corresponding impedances at the fundamental and second harmonic. With knowledge of the impedance environment, and the assumed current waveform, (3) can be evaluated to determine whether it has a positive or negative value. Fig. 8(a) and (b) show how this calculation can be plotted on an impedance plane; in this case, we vary the fundamental impedance (hence, the  $V_{1r}$  and  $V_{1q}$  value) across the entire Smith Chart plane, for specific fixed values of  $Z_{2f_0}$  (hence,  $V_{2q}$ ). The shaded portions indicate the clipping regions where the voltage expression crosses zero at some point in the cycle.

The shaded regions, as shown in Fig. 8(a) and (b), thus provide a design guide as to load conditions that should be avoided in the circuit design process. The line which delineates the clipping region is called the “clipping contour.” This contour in effect shows the impedance conditions for which the voltage “grazes” zero. However, the choice of fundamental impedance will also determine the final power and efficiency. In principle, if the real part of the fundamental impedance is maintained at a constant value, equal to the device “load-line” resistance, maximum power and efficiency will be maintained [corresponding to a fixed value of  $V_{1r}$  in (3)]. This constant maximum efficiency contour is also plotted (dotted traces) in Fig. 8(a) and (b). In practice, of course, the only allowable maximum efficiency condition will be the one that sits on the “clipping contour,” which can be seen to be a singular point in each case.

Fig. 9 shows how the clipping contour changes as the value of second harmonic reactance is varied over the class-J range. It is of interest to note that in practice, although the clipping process will change the assumed current waveform, and as such

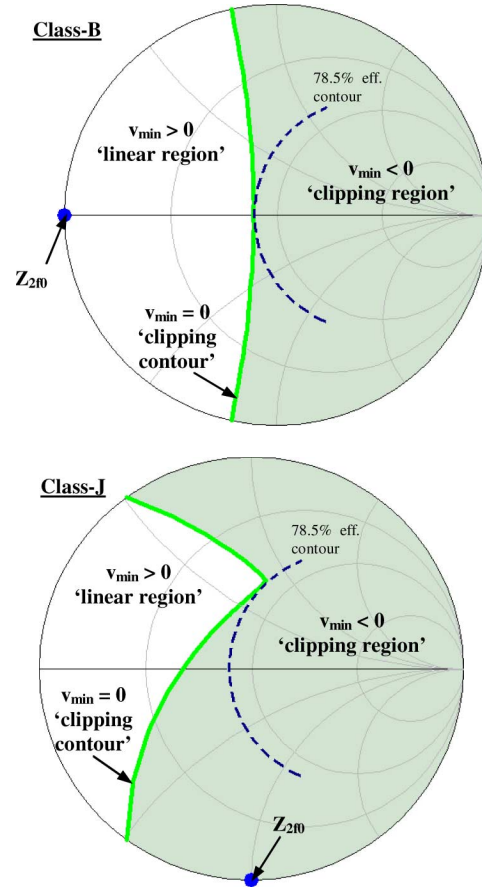


Fig. 8. (a) Class-B “clipping contour” (solid trace) indicating fundamental loads for “zero-grazing”  $v_{\min}$  condition, with “clipping region” shaded. 78.5% efficiency contour (dotted trace) also shown, indicating an optimum load for linearity and efficiency. (b) Class-J “clipping contour” (solid trace) indicating fundamental loads for “zero-grazing”  $v_{\min}$  condition, shaded “clipping region” and optimum load for class-J linearity and efficiency.

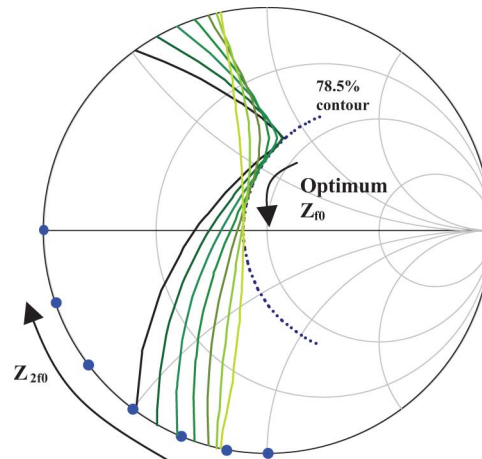


Fig. 9.  $v_{\min} = 0$  “clipping contours” indicating optimum fundamental load for efficiency, as second harmonic load impedance is varied between the class-B and class-J conditions.

the power and efficiency can no longer be simply related to the value of  $V_{1r}$  in (3), the continuation of the maximum efficiency condition into the “clipping region” can often be observed in practice. The plots in Figs. 8 and 9 define a design methodology for obtaining the best efficiency without forcing the de-

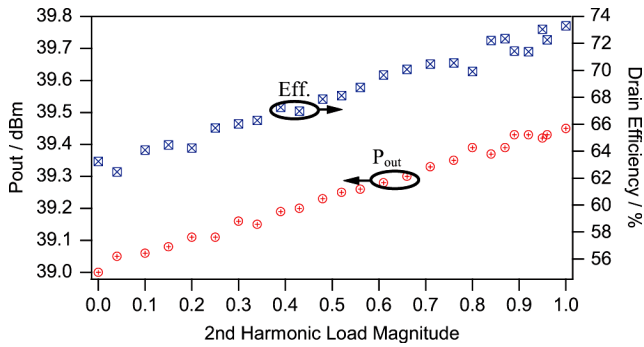


Fig. 10. Measured effect of the real component of second harmonic load on class-J output power and efficiency.

vice output voltage to “graze” zero and thus display highly non-linear, clipped behavior. To the best of our knowledge, this is the first time such a methodology has been defined for high efficiency RFPAs, and is proposed as an essential element in the design process for broader-band, high-efficiency PA design.

*C. Practical Verification of Class-J Mode in High Power Devices—Effect of Second Harmonic (LP Measurements)*

Since for a broadband PA design—and especially PAs covering octave bandwidths—the high-end fundamental impedance tends towards the second harmonic impedance at the low-end of the band, it was necessary to observe the effect that a non-ideal (i.e., not purely reactive) second harmonic load impedance has on class-J efficiency [17]. This was carried out with a fixed fundamental load of  $(30+j30)\ \Omega$  ( $I_{gen.-plane}$ ), fixed third harmonic impedance of  $50\ \Omega$  (package-plane) and for a device bias condition of  $I_{dsq} = 100\ \text{mA}$  (deep AB, approximately 5%  $I_{dss}$ ).

The results in Fig. 10 show a 10% decrease in efficiency, and almost 0.5 dB reduction in output power as the magnitude of the second harmonic load impedance is varied from 1 to 0 at the  $I_{gen.-plane}$ . Although at first glance this result shows substantial degradation in performance, there is also the indication that the transition between the fundamental load and second harmonic load impedance across an octave bandwidth can be implemented in such a way as to not dramatically degrade the efficiency performance of a class-J PA operating across this frequency range, for example; a second harmonic reflection coefficient of magnitude 0.5 would suggest just 5% drop in efficiency and 0.25 dB drop in output power, whilst still being a suitable fundamental load for this device if combined with a reactive impedance component.

*D. Practical Verification of Class-J Mode in High Power Devices—Improved Class-J Design Space LP Results*

By following investigations in [5] and simulation findings in Section IV-B the second harmonic load impedance was varied between  $+165^\circ$  and  $-105^\circ$  at the  $I_{gen.-plane}$  (done so through the use of output parasitic de-embedding), with magnitude 0.95 in each case. The optimum fundamental load for peak efficiency was targeted. The results of this are shown in Fig. 11, and have been carried out at a fundamental frequency of 1.8 GHz.

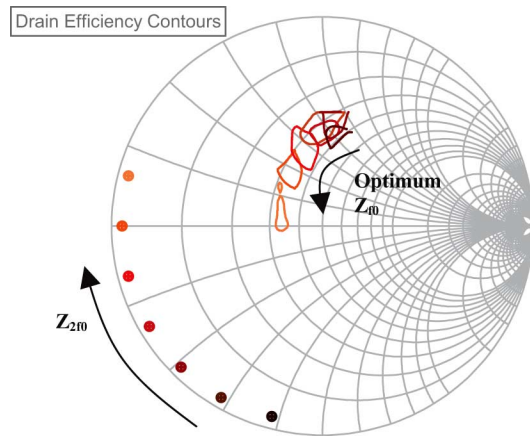


Fig. 11. Mapping the optimum (top 2%) efficiency contour as a function of changing second harmonic load impedance— $I_{gen.-plane}$  impedances shown.

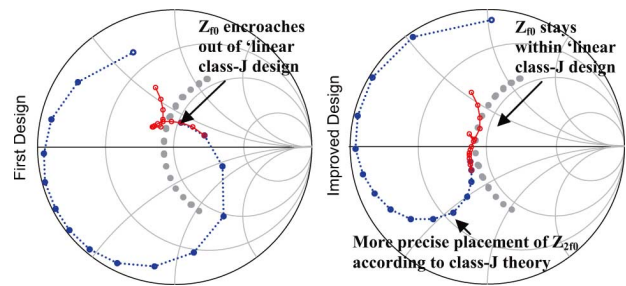


Fig. 12. (Right) Second iteration of class-J output matching compared with (left) first initial design, showing fundamental (solid line) and second harmonic (dotted line) load impedances between fundamental bandwidth of 1.2–2.6 GHz.

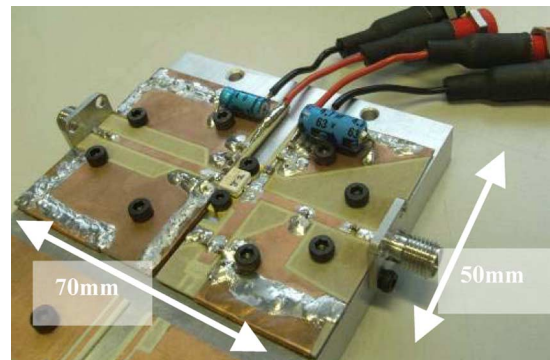


Fig. 13. Improved realized class-J amplifier.

The measured results in Fig. 11 show reasonable agreement with the theoretical analysis of class-J and the proposed “design space” for continuous high efficiency performance, as the second harmonic and fundamental load impedances are allowed to vary away from the class-B case. Since the same theory can be applied to the “complimentary” class-J\* mode, corresponding to inductive second harmonic terminations, the potential for a broadband high efficiency PA is clear.

V. ENHANCED DESIGN FOLLOWING EXTENDED THEORY

A. Redesigning the Class-J Output Matching Network

Using the analysis found/developed in the previous section, an iteration of the initial matching network, using the same

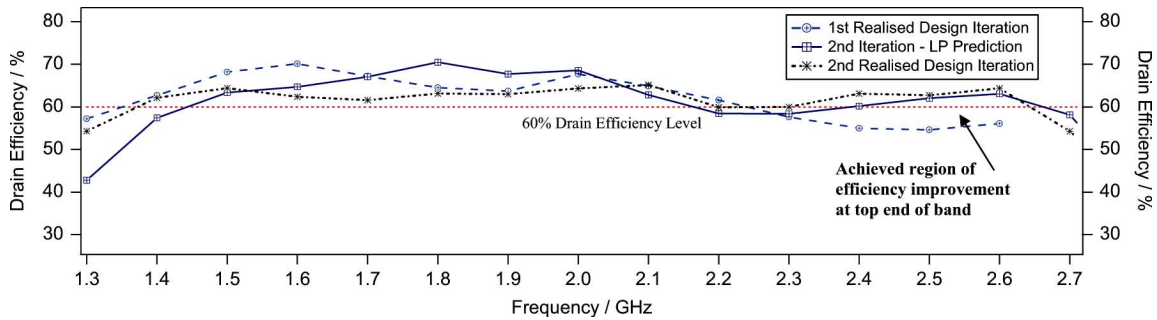


Fig. 14. Prediction and measurement of PA efficiency performance with enhanced output matching, compared with first class-J PA design performance.

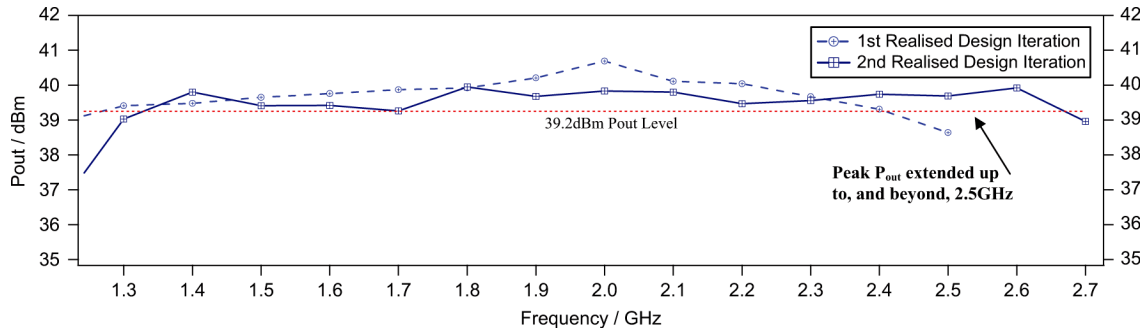


Fig. 15. Broadband measurement of PA output power performance with enhanced output matching, compared with first class-J PA design iteration.

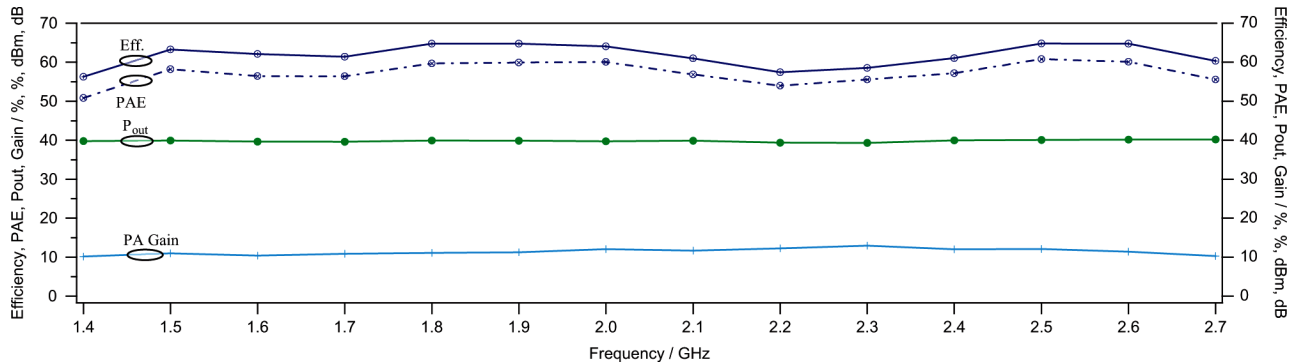


Fig. 16. Broadband measurement of PA performance with enhanced output matching, and broadband input matching.

architecture as previous (see Fig. 4), was made in line with the intention of “moving” the fundamental loads that were encroaching on the “clipping,” or nonlinear region of the Smith Chart, and more precise placement of the second harmonic load, in particular regards to the phase. This second design iteration is shown by the *s*-parameters of Fig. 12, giving a comparison with the first output matching design.

In the same way as previous, this improved design, following extended theoretical-based analysis, was used to predict the performance that could be expected from the PA by using active load-pull. These results showed improvement in efficiency at the higher frequency end of the bandwidth of operation as desired, above 2.2 GHz, and as shown in Fig. 14.

### B. Measured PA Performance Following Improved Output Matching Network Design

In characterizing the second realized PA, power sweeps were again conducted at 100 MHz frequency spacing and the efficiency at P2 dB (2 dB gain compression point) was recorded, along with the output power and amplifier gain. These sets of results are displayed also in Figs. 14 and 15, along with the first

design iteration results for comparison. Measured P2 dB output power, as in Fig. 15, indicates the flat characteristic associated with this broadband design, at a value of  $39.5 \pm 0.5$  dBm (approximately 9–10 W). The improvement in drain efficiency of the second iteration PA is evident in Fig. 14 between 2.3 and 2.6 GHz, with up to 8% improvement obtained at 2.5 GHz.

Fig. 13 shows the improved class-J amplifier.

## VI. INPUT MATCHING AND AFFECT ON PA PERFORMANCE

For comparison purposes the PA was measured with the same input impedance as the device was measured during the load-pull design stage; with a broadband  $50 \Omega$  impedance and not for best gain.

Following the performance characterization in the previous sections attention turned to improving the input match across the frequency band of 1.4–2.6 GHz and hence improve power-added efficiency (PAE). The applied input matching resulted in the PA performance shown in Fig. 16, including PAE. Here, gain of between 10.2–12.2 dB across the bandwidth of 1.4–2.7 GHz has been observed and hence has resulted in an improved PAE of more than 50% across the same bandwidth.

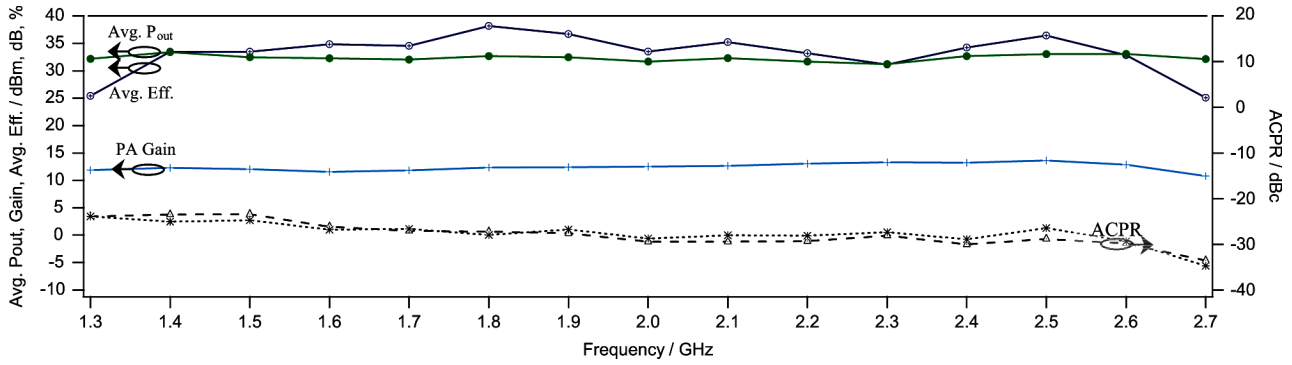


Fig. 17. Broadband PA linearity (with broadband input matching) characterized under stimulus of 5 MHz BW, 8.51 dB PAR, WCDMA signal.

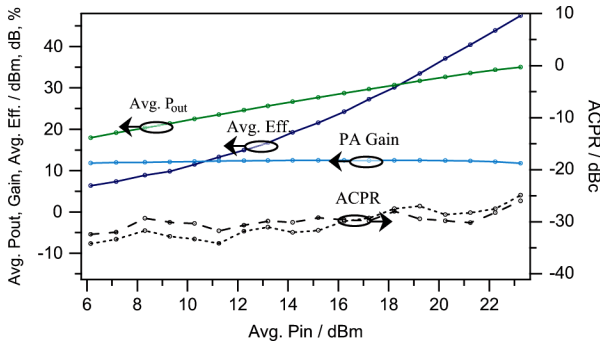


Fig. 18. Input matched class-J PA performance with a power-swept 5 MHz BW, WCDMA signal at center frequency of 2.0 GHz.

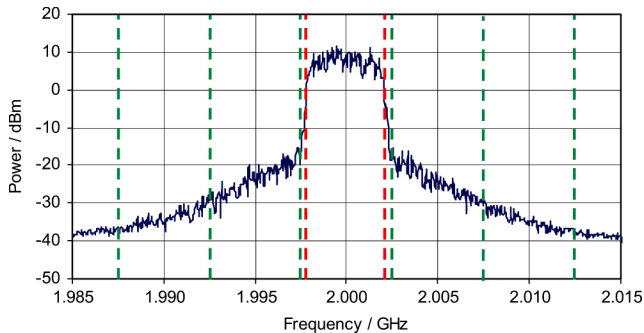


Fig. 19. Output spectrum from class-J PA, measuring ACP for a 3.84 MHz WCDMA signal at center frequency 2.0 GHz, and at 40% average efficiency.

VII. PA LINEARITY AND ACPR CHARACTERISTICS

Very high efficiency PAs can be prone to very nonlinear characteristics which present users with a difficult, if not impossible, task of predistorting the PAs to meet communication system standards. ACPR, without any form of predistortion, was measured across the frequency range of 1.3–2.7 GHz and results in Fig. 17 show average power, efficiency, and gain as well as worst-case upper and lower channel ACPR with drive power sufficient to cause 2 dB peak compression. At a CF (center-frequency) of 2.0 GHz, the same PA characteristics are plotted in Fig. 18 for a range of drive powers, while Fig. 19 shows a captured spectrum at an average efficiency of 40% at the same CF. The modulated signal applied, in order to characterize the PA linearity, was a WCDMA signal of 3.84 MHz signal bandwidth and 8.51 dB PAR. ACPR of close to -30 dBc has been measured between 1.7–2.7 GHz, decreasing to approximately -25 dBc below 1.7 GHz; this at the same time as the PA operating at more than 30% average efficiency.

The relative symmetry of the upper and lower ACP sidebands in Fig. 19 implies minimal memory effects and good potential for predistortability using techniques such as those presented in [6] and [7]. We attribute this excellent “raw” linearity performance to the design methodology described in Section IV-B.

VIII. CONCLUSION

A fully realized class-J amplifier has demonstrated high efficiency operation across a substantial bandwidth. Following on from a previous paper, further newly presented theory of class-J as a broadband mode has been applied in improving an initial output matching network design. Load-pull results and simulation analysis have justified these changes and enabled a second design and fabrication of an output matching network which has shown improved efficiency performance with frequency. The use of active harmonic load-pull and waveform measurement capability has shown, throughout this research, to be a powerful tool in developing real PA designs using theory specific to the class-J mode of operation. Efficient PA performance has been measured across a bandwidth of 1.4–2.6 GHz (60% bandwidth, centered at 2 GHz) whilst showing ACPR of approximately 25–30 dBc across the entirety of this bandwidth at the measured P2 dB compression level.

ACKNOWLEDGMENT

The authors would like to thank R. Pengelly (Cree Inc.) for the supply of GaN devices used in this work.

REFERENCES

- [1] S. C. Cripps, *RF Power Amplifiers for Wireless Communications*, 2nd ed. Boston, MA: Artech, 2006.
- [2] P. Colantonio, F. Giannini, G. Leuzzi, and E. Limiti, “High efficiency low-voltage power amplifier design by second harmonic manipulation,” *Int. J. RF Microw. Comput.-Aided Eng.*, vol. 10, no. 1, pp. 19–32, Jan. 2000.
- [3] P. Colantonio, F. Giannini, G. Leuzzi, and E. Limiti, “Theoretical facet and experimental results of harmonic tuned PAs,” *Int. J. RF Microw. Comput.-Aided Eng.*, vol. 13, no. 6, pp. 459–472, Nov. 2003.
- [4] P. Wright, J. Lees, P. J. Tasker, J. Benedikt, and S. C. Cripps, “An efficient, linear, broadband class-J-mode PA realised using waveform engineering,” in *IEEE MTT-S Int. Microw. Symp. Dig.*, 2009, pp. 653–656.
- [5] S. C. Cripps, P. J. Tasker, A. L. Clarke, J. Lees, and J. Benedikt, “On the continuity of high efficiency modes in linear RF power amplifiers,” *IEEE Microw. Wireless Compon. Lett.*, vol. 19, no. 10, pp. 665–667, Oct. 2009.
- [6] J. Goodman, B. Miller, G. Raz, and M. Herman, “A new approach to achieving high-performance power amplifier linearization,” in *Proc. IEEE Radar Conf.*, Apr. 2007, pp. 840–845.

- [7] G. Montoro, P. L. Gilabert, E. Bertran, A. Cesari, and D. D. Silveira, "A new digital predictive predistorter for behavioral power amplifier linearization," *IEEE Microw. Wireless Compon. Lett.*, vol. 17, no. 6, pp. 448–450, Jun. 2007.
- [8] J. Benedikt, R. Gaddi, P. J. Tasker, M. Goss, and M. Zadeh, "High power time domain measurement system with active harmonic load-pull for high efficiency base station amplifier design," in *IEEE MTT-S Int. Microw. Symp. Dig.*, 2007, pp. 1459–1462.
- [9] P. Colantonio, F. Giannini, R. Giofrè, and L. Piazzon, "High efficiency ultra-wide-band power amplifier in GaN technology," *IEEE Electron. Device Lett.*, vol. 44, no. 2, pp. 130–131, Feb. 2008.
- [10] A. Sheikh, P. J. Tasker, J. Lees, and J. Benedikt, "The impact of system impedance on the characterization of high power devices," in *Proc. 37th Eur. Microw. Conf.*, Oct. 2007, pp. 949–952.
- [11] F. H. Raab, "Class-E, class-C, and class-F power amplifiers based upon a finite number of harmonics," *IEEE Trans. Microw. Theory Tech.*, vol. 49, no. 8, pp. 1462–1468, Aug. 2001.
- [12] H. M. Nemati, C. Fager, M. Thorsell, and H. Zirath, "High-efficiency LDMOS power-amplifier design at 1 GHz using an optimized transistor model," *IEEE Trans. Microw. Theory Tech.*, vol. 57, no. 7, pp. 1647–1654, Jul. 2009.
- [13] T. B. Mader, E. W. Bryerton, M. Markovic, M. Forman, and Z. Popovic, "Switched-mode high-efficiency microwave power amplifiers in a free-space power-combiner array," *IEEE Trans. Microw. Theory Tech.*, vol. 46, no. 10, pp. 1391–1398, Oct. 1998.
- [14] P. Wright, A. Sheikh, C. Roff, P. J. Tasker, and J. Benedikt, "Highly efficient operation modes in GaN power transistors delivering upwards of 81% efficiency and 12 W output power," in *IEEE MTT-S Int. Microw. Symp. Dig.*, 2008, pp. 1147–1150.
- [15] C. Roff, J. Benedikt, P. J. Tasker, D. J. Wallis, K. P. Hilton, J. O. Maclean, D. G. Hayes, M. J. Uren, and T. Martin, "Analysis of DC-RF dispersion in ALGaIn/GaN HFETs using RF waveform engineering," *IEEE Trans. Electron Devices*, vol. 56, no. 1, pp. 13–19, Jan. 2009.
- [16] A. Grebennikov and N. O. Sokal, *Switchmode RF Power Amplifiers*. New York: Newnes, 2007.
- [17] C. Roff, J. Benedikt, and P. J. Tasker, "Design approach for realization of very high efficiency power amplifiers," in *IEEE MTT-S Int. Microw. Symp. Dig.*, 2007, pp. 143–146.



**Peter Wright** received the B.Eng. degree in electronic engineering from Cardiff University, Cardiff, U.K., in 2006, where he is currently pursuing the Ph.D. degree in electronic engineering from the Centre for High Frequency Engineering.

His research interests include the application of RF waveform engineering for PA design, in particular the development of design methodologies for the efficiency enhancement of RFPAs.



**Jonathan Lees** received the B.Eng. degree in electronic engineering from Swansea University, U.K., in 1992, and the M.Sc. and Ph.D. degrees from Cardiff University, Cardiff, U.K., in 2001 and 2006, respectively.

From 1992 to 2002, he was with QinetiQ, where he developed global positioning and advanced optical instrumentation tracking systems. He was a Chartered Engineer (MIET). He is now a Research Associate with the Centre for High Frequency Engineering, Cardiff University, where his research

continues into power amplifier design, load-pull, and large signal measurement systems.



**Johannes Benedikt** received the Dipl.-Ing. degree in electrical engineering from the University of Ulm, Ulm, Germany, in 1997, and the Ph.D. degree from Cardiff University, Cardiff, U.K., in 2002.

During this time, he took on an additional position as a Senior Research Associate with Cardiff University starting in October 2000, where he supervised a research program with Nokia on RFPAs. In December 2003, he was appointed a Lecturer with Cardiff University, where he was responsible for furthering research in the high-frequency area. His

main research focus is on the development of systems for the measurement and engineering of RF current and voltage waveforms and their application in complex PA designs.



**Paul J. Tasker** (M'88–SM'07) received the B.Sc. degree in physics and electronics and Ph.D. degree in electronic engineering from Leeds University, U.K., in 1979 and 1983, respectively.

From 1984 to 1990, he worked as a Research Associate with Cornell University, Ithaca, NY, with Prof. L. Eastman, where he was involved in the early development of HFET transistors. From 1990 to 1995, he was a Senior Researcher and Manager with the Fraunhofer Institute for Applied Solid State Physics (IAF), Freiburg, Germany, where he was responsible

for the development of millimeter wave MMICs. He joined the School of Engineering, Cardiff University, Cardiff, U.K., as a Professor in the summer of 1995, where he has been establishing the Cardiff University and Agilent Technology Centre for High Frequency Engineering. The center's research objective is to pioneer the development and application of RF I-V waveform and engineering systems, with a particular focus on addressing the PA design problem. He has contributed to over 200 journal and conference publications and given a number of invited conference workshop presentations.

Dr. Tasker has been appointed as an IEEE Distinguished Microwave Lecturer for the term of 2008–2010.



**Steve C. Cripps** received the Ph.D. degree from Cambridge University, Cambridge, U.K.

He worked for Plessey Research on GaAsFET hybrid circuit development. Later, he joined Watkins-Johnson's Solid State Division, Palo Alto, CA, and has held Engineering and Management positions at WJ, Loral, and Celeritek. During this period, he designed the industry's first 2–8 and 6–18 GHz 1 watt solid-state amplifiers. In 1983, he published a technique for microwave power amplifier design, which has become widely adopted

in the industry. In 1990, he became an independent consultant and was active in a variety of commercial RF product developments, including the design of several cellular telephone PA MMIC products. In 1996, he returned to the U.K., where his consulting activities continue to be focused in the RFPAs area. He has recently been appointed a Professorial Research Fellow at Cardiff University, U.K. He has recently authored a second edition of his best selling book, *RF Power Amplifier Design for Wireless Communications* (Artech House, 2006).

Dr. Cripps was a recipient of the 2008 IEEE Microwave Applications Award. He is currently vice-chair of the High Power Amplifier Subcommittee of the Technical Coordination and Technical Program Committees of the IEEE Microwave Theory and Techniques Society, and writes the regular "Microwave Bytes" column in the *IEEE Microwave Magazine*.